RESEARCH ARTICLE

DELINEATION OF AIRBORNE MAGNETIC AND RADIOMETRIC STRUCTURES ASSOCIATED WITH GOLD MINERALIZATION OF MINNA AND ITS ENVIRONS, NORTHCENTRAL NIGERIA

Saleh A[a*], Udensi E.E.[b], Salako K.A.[c] and Unuevho, C.I.[d]

[a]*Physics Unit, School Preliminary and Continuing Education, Ibrahim Badamasi Babangida University Lapai*
[b]*Department of Physics, Federal University of Technology Minna*
[c]*Department of Geophysics, Federal University of Technology Minna*
[d]*Department of Geology, Federal University of Technology Minna*
*Corresponding Author E-mail: aliyusaleh44@gmail.com

ARTICLE DETAILS

ABSTRACT

This study utilized the interpretation of the airborne magnetic and radiometric data to delineate the potential structures that are associated with gold mineralization of the Minna and its environs, Northcentral Nigeria. The total field anomaly data was reduced to pole and upward continued in a bid to well positioned and enhanced the shallow (high pass) magnetic structures. The high pass structural lineaments were extracted and the resulting prominent E-W and NE-SW tectonic trends were revealed which are perhaps related to Eburnean (D_1) and Pan-African (D_2) deformation events respectively. Subsequently, numerous regions with relatively high degree of faulting and shearing effects were unraveled from the line density analysis of the high pass lineaments. The 3-D Euler deconvolution technique provides a synonymous trend pattern with the HP lineaments as well as estimate the depth extents to the potential structures with values varying between 82.7 and 211.9 m. It was found that the mineralized structures associated with gold over the study area interact with the hydrothermal fluids alongside/adjacent to the structurally deformed (relatively high degree of faulting and shearing effects) regions. The observed regions with coincident, of the hydrothermally altered and structurally deformed are therefore marked as the resourceful, structures for gold mineralization. Hence, the derived evidence from this study has updated the information on the structures that are associated with gold mineralization and also acts a mitigation major against the indiscriminate excavations of the studied region.

KEYWORDS

Gold, Structures, Mineralization, Minna, Magnetic, Radiometric

1. INTRODUCTION

The search for geologic structures that are associated with gold mineralization over Minna and its environs has been a major challenge for the artisanal mining activities. This is because, artisanal mining activities over the study area are generally affected by inadequate financial and mining know-how of their main target (gold). As such, pre-exploration information of their main target such as; the trends and precise location of the mineralized structures, depth extent to the delineated structures as well as the hydrothermally altered zones remains anonymous. These artisan miners in their effort to locate their main target, usually employs trial and error excavation techniques without considering the environmental ramifications. In general, gold deposit occurs alongside other heavy metals such as; copper, nickel, lead, tin, zinc, cobalt, among others can perhaps pose serious health threat when illogically released into the environments. However, airborne magnetic and radiometric data were used in this study because, they are cheap and rapid geophysical survey techniques. In particular, airborne magnetic method measures the differences in the earth magnetic field due to induced and remnant magnetization in rock units (Telford et al., 1990). The magnetic technique probes the earth crust for possible structures that are associated with gold mineralization (Boadi et al., 2013; Ejepu et al., 2018). The corresponding

radiometric method measures the distribution of the uranium (U), thorium (Th) and potassium (K) in the earth crust (Silva et al., 2003). The radiometric data has been extensively used in detecting different lithologic units and hydrothermally altered zones (Jaques et al., 1997; Elkhateeb and Abdellatif, 2018).

Numerous studies have been carried out in some part of the study area. For example; a group of researchers interpreted the in-situ magnetic data and determined the structures associated with gold deposits over Gwam area Northcentral Nigeria (Ishalu and Tsepav, 2018). A previous researcher delineated the prospective gold mineralised zones of Kwakuti Northcentral Nigeria using airborne radiometric and magnetic data (Ejepu et al., 2018). A researcher interpreted the geologic structures of Allawa Northcentral Nigeria using aeromagnetic data (Saleh et al., 2020). A study employed airborne magnetic and radiometric data to delineate the structures associated with gold deposits over Bida and Zungeru Northcentral Nigeria (Aliyu et al., 2021). In view of this, the aforesaid studies could neither classify the structurally deformed regions nor correlate the deformed regions with the depicted hydrothermally altered zones. Since, geologic structures associated with gold mineralization are basically controlled by three major mechanisms namely; lithological settings, hydrothermal alterations and structural deformations (Sillitoe,

1999). These necessitate the need to map the geologic structures (such as faults, folds, contacts, shear zones among others) that are associated with gold mineralization as well as estimate their respective depth extents using interpretation techniques such as; reduction to pole (RTP), high pass (HP), Centre for exploration targeting (CET), line density analysis and 3-D Euler deconvolution. The ratio of potassium to thorium (K/Th) anomaly of the airborne radiometric data provides a good estimate of the hydrothermally altered zones (Wemegah et al., 2015). Hence, the present study provides a new paradigm into the potential structures associated with gold mineralization and also act as a mitigation major against the indiscriminate trial and error excavations over Minna and its environs.

1.1 Location and Geology Settings of the Study Area

The study area is bounded by latitudes 9o to 10o and longitudes 6o to 7o E covering Zungeru, Minna, Bida and Paiko areas with an estimated total area of 12100 km2. The regional geological setting of Nigeria (Figure 1) has categorized the study area is into; Cretaceous sediments, Archean basement and Neoproterozoic granitoids (older granites) formations (Benkhelil et al., 1998; Obaje, 2009; Salawu et al., 2021).
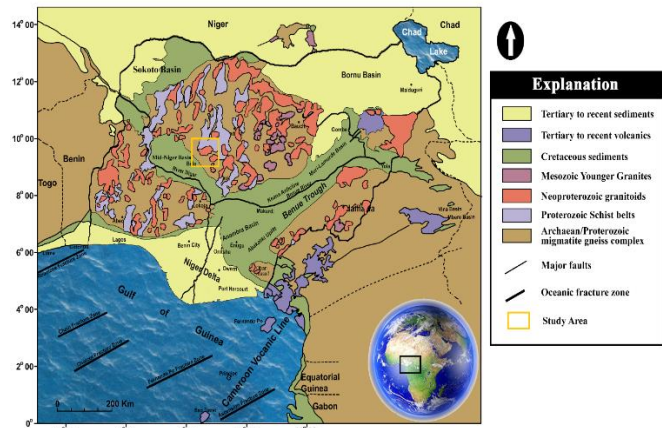

Figure 1: The Nigeria geological map and its environs showing the study area indicated with green square box (Modified after Benkhelil et al., 1998; Salawu et al., 2021)

The south-western part of the study area makes a portion of the northern Nupe cretaceous sediment formations, which constitutes; silicified rocks and large quartz veins, Nupe sandstones and siltstones (Figure 2). Elsewhere, with the exception of the south-western flank of the study area is covered by the Crystalline basement complex (CBC). The CBC segments of the study area like the regional geology of Nigeria is made up of; Archean migmatites-gneiss complex, Proterozoic schist belts and Neoproterozoic granitoids. The Archean migmatites-gneiss complex consists of numerous assemblages including; migmatites, paragneisses, orthogneises and a sequence of basic and ultrabasic metamorphosed rocks (Obaje, 2009). Figure 2, reveals numerous assemblages (amphibolites, mylonites and mylonites interlaid with amphibolites) which are observed

in the north-western plank of the study area. The observed assemblages are due to the fractional melting along most of the rock formations displaying medium to upper amphibolite facies metamorphism. These has resulted to recrystallization of many of the constituent minerals of the Archean migmatite-gneiss complex from the Eburnean 2700 (Ma) to Pan-African 600 600 (Ma) ages (Obaje, 2009). The Proterozoic schist belts infolded into the migmatite-gneiss-quartzite complex and constitutes; pelitic schists, banded iron formation, phyllites, coarse to fine grained clastics, carbonate rocks and mafic metavolcanics (amphibolites) (Woakes et al., 1987).
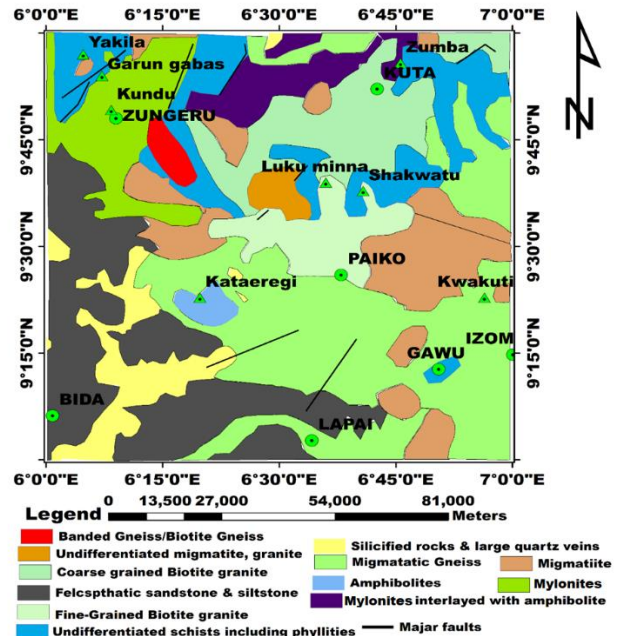

Figure 2: The geological map of the study area (modified after NGSA, 2010)

2. MATERIALS AND METHODS

2.1 Airborne Magnetic and Radiometric Data

Airborne magnetic data was acquired from the Nigeria Geological Survey Agency (NGSA). The data was obtained using an aircraft which was flown in the NW-SE direction, 500 m line spacing, mean sensor terrain clearance of 80 m and tie lines interval of 2000 m interval were used (NGSA, 2010). The acquired airborne magnetic data were corrected for diurnal variation and International Geomagnetic Reference Field (IGRF) 2005 model as shown in Figure 3a. The airborne radiometric data was micro-levelled and the resulting apparent residual errors were subtracted (Figures 3b, c and d).
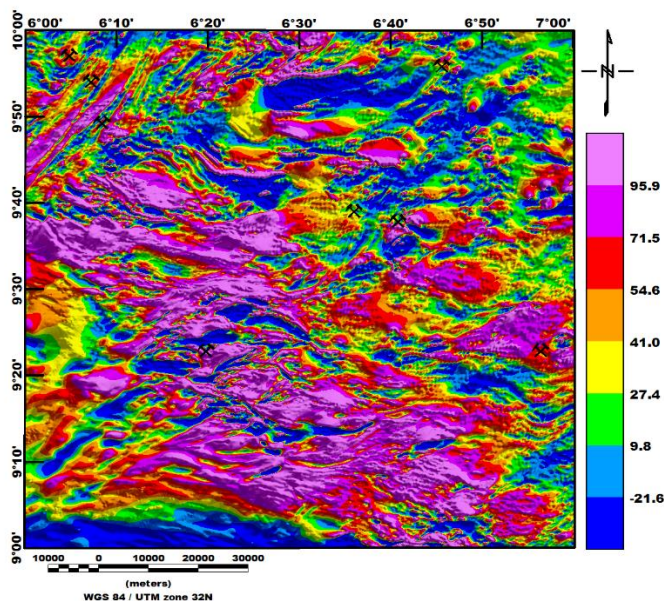

Figure 3a: Total field anomaly map of the study area

2.2 Airborne Magnetic Data Processing

(a) the total field anomaly (TFA) data (Figure 3a) was reduced to pole (RTP) (b). the RTP anomaly data were upward continued at height of 150 m to produce the high pass (residual) anomaly data (c). the residual anomaly was subjected to the high pass (HP) filter to enhance the near surface structures (d). HP anomaly was subjected to automatic lineament extraction analysis using the Centre for Exploration Targeting (CET) (e). the HP lineaments serves as input for the line density computations in an attempt to differentiate between high, moderate and low near surface deformed zones (f). the 3-D Euler deconvolution method was used to estimate the depths to the magnetic lineaments identified from the HP anomalies. Hence, the theories of the adopted magnetic data interpretation are.

2.2.1 3-D Euler Deconvolution (ED)

The high pass (HP) anomaly data was subjected to the 3-D Euler deconvolution (ED) method in order to estimate the depths and locations of the near surface structures. The ED method is independent on the direction of magnetization. The 3-D Euler deconvolution is based on the Euler's homogeneity equation (Thompson, 1982) given as thus:

$$(x - x_0)\frac{\partial F}{\partial x} + (y - y_0)\frac{\partial F}{\partial y} + (z - z_0)\frac{\partial F}{\partial z} = N(B - F) \quad (1)$$

Where, x_0, y_0 and z_0 are the position or coordinate of the top magnetic source, (x, y, z) are the location of the field measurement, HP anomaly value, B is the background field, $\frac{\partial T}{\partial x}$, $\frac{\partial T}{\partial y}$ and $\frac{\partial T}{\partial z}$ are the derivative of the total field values T and N is the degree of homogeneity known as structural index (SI). The SI measures the rate of change with distance of a field (Thompson, 1982).

2.3 Airborne radiometric data processing

The airborne radiometric data potassium (K) and thorium (Th) anomalies (Figure 3b and c) were used for the hydrothermal alteration mapping (a). the regions with relatively high K/Th ratio values were used to delineate the hydrothermally altered zones. The theory of the method is given as thus;

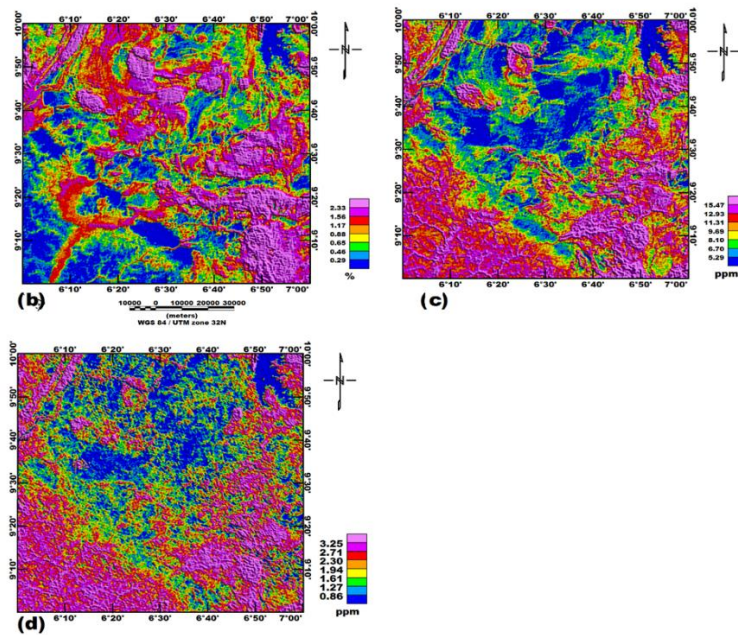$$Hydrothermal\ \ alteration = \frac{K}{Th} \quad (2)$$

Figure 3: Airborne radiometric anomaly maps of the study area (b) Potassium (c) Thorium (d) Uranium

3. RESULTS AND DISCUSSION

3.1 Interpretation of the Reduce to pole (RTP) anomaly map

The reduce to pole (RTP) anomaly transformation was carried out on the IGRF reduced 33,000 nT total field anomaly data (Figure 3a). The RTP map (Figure 4) displays a shift in the magnetic sources anomalies in contrast to the TFA data (Figure 3a). Evidently, areas of high magnetic signatures on the RTP map (Figure 4) are seen as areas of low magnetic signatures (Figure 3a) and vice versa.
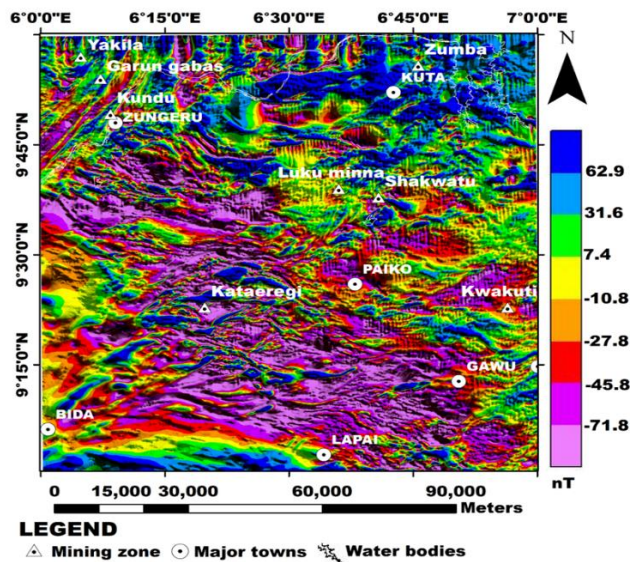

Figure 4: The reduced to pole anomaly map obtained from the total field anomaly

The RTP map (Figure 4) portrays magnetic high and low anomalies in different shapes within the study area. The regions characterized by high (strong positive) magnetic signatures are represented in red to pink colours with values in the range of 7.4 to 62.9 nT. However, the areas of high magnetic signature are more prominent at the NNW (Yakila, Garun Gabas, Kundu and Zungeru), NNE (Kuta and Zumba), mid north (Luku Minna and Shakwatu) to SE (Gawu and Lapai) parts of the study area. These high magnetic signatures are characterized by NE-SW and E-W trends within the crystalline basement complex in contrast to the geological setting (Figures 2 and 3). Equally, regions occupied by yellow to blue colours with values in the range of -27.8 to -77.8 nT, suggest broad low (strong negative) magnetic signatures. The observed low magnetic signatures are more prominent in the northern, central (Kataeregi and Paiko) and SSW (Bida)-SSE (Lapai) portions of the study area. The low magnetic signatures have similar series of E-W and NW-SE trends with the high magnetic signatures. The low magnetic signatures are perhaps due to sedimentary rock units such as; sandstones, quartz, siltstones and carbonates rocks in comparison with the geological setting (Figures 2 and 3) of the study area.

3.2 Interpretation of the RTP high pass anomaly map

The RTP anomaly data was upward continued at a height of 150 m. The upward continued anomaly grid was subtracted from the TFA anomaly (Figure 3a) to obtain the high pass (HP) anomaly (Figure 5). The HP anomaly map reveals the short wavelength signatures which were masked up by the long wavelength magnetic sources.
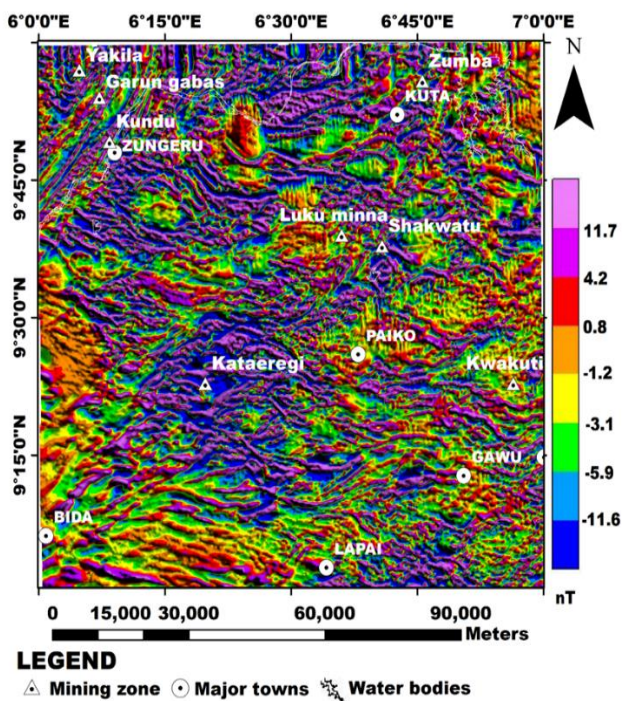

Figure 5: High pass map obtained from the reduced to pole anomaly of the study area

The HP further reveals the subdued near surface structures at the expense of the deep magnetic sources. Evidently, shallow (near surface) geologic structures over the study area were better enhanced in contrast to those observed in the RTP anomaly map in figure 4. The HP anomaly map reflects strong positive and negative magnetic signatures in blue to pink colours with values that varies between -11.6 and 11.7 nT respectively. These strong positive and negative HP signatures are more prominent along NNW (Yakila, Garun Gabas, Kundu and Zungeru), NNE (Kuta and Zumba), mid north (Luku Minna and Shakwatu), mid-south (Lapai), ESE (Izom) and central (Kataeregi and Paiko) parts of the study area are characterized by relatively elevated HP magnetic signatures. These relatively HP magnetic signatures have significant magnetic susceptibility variations and thus produced detectable magnetic structures over the study area. The relatively low magnetic signatures are prominent along the SSW (Bida)-SSE (Lapai) portions of the study area are due to sedimentary formations over the study area.

Figure 6a reveals the near surface structures (lineaments) which act as the potential host of mineralized deposits, were extracted from the HP anomaly. The observed lineaments were extracted using the Centre for Exploration Targeting (CET) menu on the Geosoft Geophysical package.
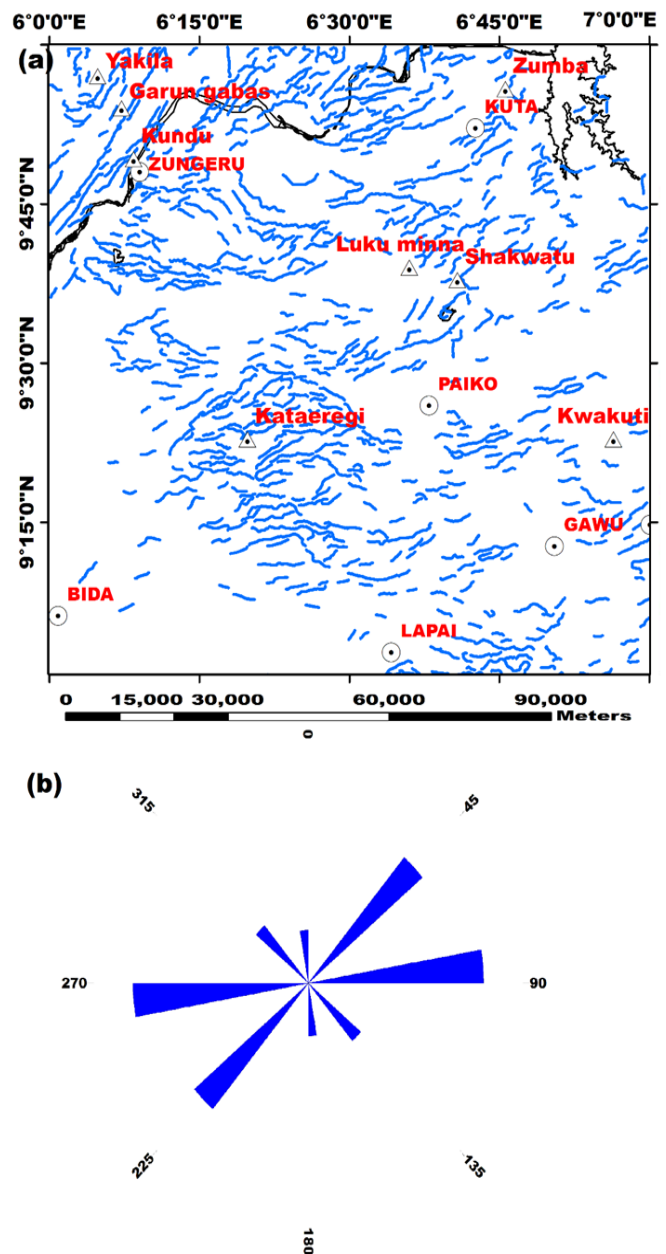

Figure 6: (a) Structural map of the study area produced from the extracted HP lineaments (b) Rose diagram produced from HP lineament

Several linear and curvilinear geologic structures (folds, faults, fractures, shear zones etc.) were unveiled. Along these geologic structures mineralized deposit (such as gold among others) in form of hydrothermal fluids are perhaps transported and accumulated. The Rose diagram (Figure 6b) reveals that the extracted HP lineaments are primarily oriented in the NE-SW and E-W directions. The observed prominent E-W and NE-SW trends are related to the Eburnean (D1) and Pan-African (D2) deformations events respectively. The observed D1 and D2 tectonic deformation events from this study is in conformity with the earlier studies who worked in portions of the study area (Ejepu et al., 2018; Saleh et al., 2020).

The resulting HP lineament were subjected to the line density computation (Figure 6c) which classified the structurally deformed regions into four different colour zones; red, yellow, magenta and blue. These colours signify the regions of low, moderate, high and very high lineament density respectively. The regions of moderate to very high lineaments densities (yellow, magenta and blue colours) are dominantly observed within the amphibolite schists at Kataeregi, silicified quartz rocks at the southern part of Lapai as well as undifferentiated schist, mylonites, mylonites interlaid with amphibolites and migmatitic gneiss situated at Yakila, Garun Gabas, Kundu, Zungeru and Kuta in contrast to the geological map (Figure 2). However, areas of relatively high lineament densities somewhat coincided with the active gold mines at Kataeregi, Yakila, Garun Gabas, Kundu, Zungeru, Kuta and Shakwatu as well as delineated numerous prospective zones.
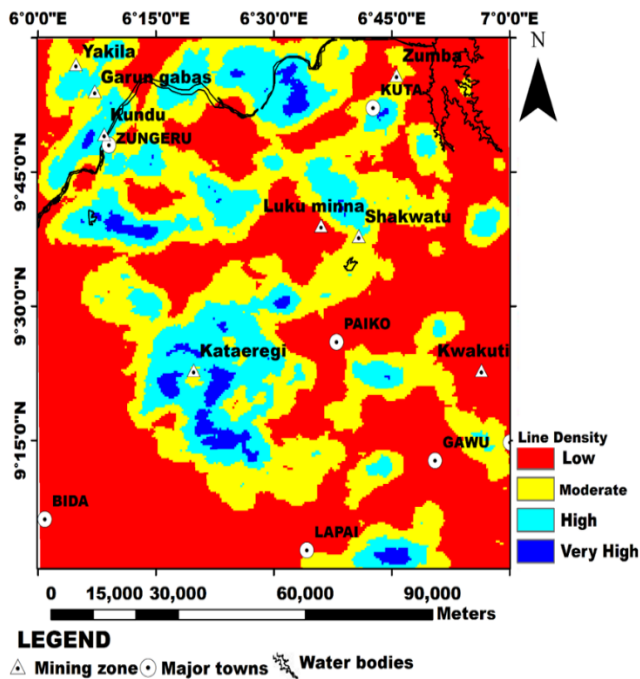
Figure 6c: High pass lineament density map of the study area

3.3 Interpretation of the HP lineaments superimposed on the 3-D Euler deconvolution map

The 3-D Euler deconvolution method was applied HP anomaly data by utilizing a window size of 6000 m width and a maximum depth tolerance of 50%. Structural index of one (1) geologic model was utilized to estimate the depths to the subsurface structures (HP lineaments) within the study area. However, the visual examination of the 3-D Euler deconvolution map (Figure 7) reveals that the estimated depths to the geologic structures varies between 82.7 and 211.9 m. The superposition of the HP lineaments on the 3-D Euler deconvolution depths solutions map (Figure 7), reveals a good correlation. The clusters of depth solutions reveal nearly similar trends with the near surface structures.
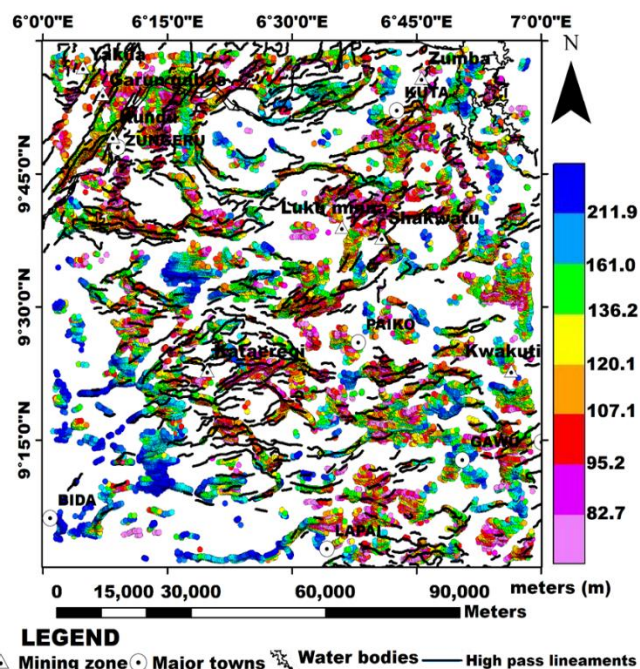

Figure 7: 3-D Euler deconvolution depth solution with superimposed HP lineaments

3.4 Interpretation of the K/Th anomaly with superimposed HP lineaments map

Figure 8 represents the potassium to thorium (K/Th) ratio map of the study area. The K/Th anomaly map (Figure 8) produced both low to high values which varies between 0.03 in blue colour and 0.24 %/ppm in blue to pink colours respectively. The hydrothermally altered specialized zones

are usually marked by values above this range 0.17 to 0.20 %/ppm (Hoover et al., 1992). This implies that regions characterized by higher K/Th values > 0.24 %/ppm, as indicated on the legend bar (pink colour) portrays a strong indication of hydrothermal alteration. Clearly, the HP lineaments were superimposed on the K/Th anomaly map to assess the correlation that exist between the hydrothermally altered zones and the near surface HP lineaments (Figure 8). It was observed that the HP lineaments are bounded and somewhat dissected most parts of the hydrothermally altered zones.
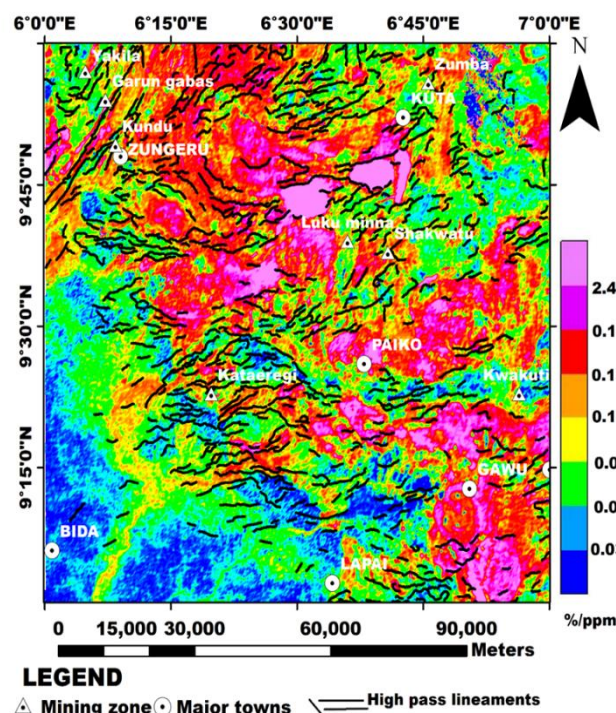

Figure 8: K/Th anomaly with superimposed HP lineaments map

The near surface structures (lineaments) were overlaid on the hydrothermally altered zones (red to pink colours) and coupled to the high magnitude of the hydrothermal alteration observed along the NNW, mid-north, central and ESE segments of the study area. The hydrothermal-auriferous fluids migrate, accumulate, penetrate and spreads even beyond the near surface lineaments brittle fault rock formations. Thus, leading to the formation of the mineralized zones of ore deposits (such as; gold) among others to intermingle with the parent rocks (protoliths) thereby resulting to hydrothermal alteration haloes and precipitation of auriferous fluids that are perhaps expressed at the NNW, mid-north, central and ESE segments of the study area. The spatial correlation of the hydrothermally altered zones and regions of the relatively high near surface line density maps (Figures 6c and 8) reveals a good correlation. Thus, implies that geologic structures associated with gold mineralization falls within the regions of strong positive and negative magnetic as well as hydrothermally altered. Hoover and Pierce (1990) described that gold among others is common in the hydrothermally altered and tectonically deformed regions.

4. CONCLUSION

Airborne magnetic and radiometric data were utilized to delineate the potential structures that are associated with gold mineralization over Minna and its environs Northcentral Nigeria. The total field anomaly data was reduced to pole and upward continued to enhanced the near surface (high pass) structures. The near surface structural lineaments were extracted from the high pass anomaly and the resulting prominent E-W and NE-SW tectonic trends were revealed which are related to Eburnean deformation (D1) and Pan-African (D2) deformation events respectively. Subsequently, the regions of various degree of faulting and shearing effects were unraveled from the line density analysis of the high pass lineaments. The depth to the potential gold mineralized structures varies between 82.7 and 211.9 m. The hydrothermally altered regions (relatively high K/Th) and the structurally deformed (relatively high faulted and sheared) zones were compared and a good correlation was observed. Thus, the study reveals that the delineated structurally deformed structures act as pathways for the migration and accumulation hydrothermally altered fluids. Therefore, gold among other deposit is found in the hydrothermal fluids alongside/adjacent to the structurally deformed regions.

REFERENCES

Aliyu, S. B., Adetona, A. A., Rafiu, A. A., Ejepu, J., Adewumi, T. 2021. Delineating and Interpreting the Gold Veins Within Bida and Zungeru Area, Niger State Nigeria, Using Aeromagnetic and Radiometric Data. Pakistan Journal of Geology, 5(2), pp. 41-50. DOI: 10.2478/pjg-2021-0006.

Benkhelil, J., Mascle, J., Guiraud, M. 1998. Sedimentary and structural characteristics of the Cretaceous along the Coˆte D'Ivoire–Ghana transform margin and the Benue trough: A comparison. In: Mascle J, Lohmann GP, Moullade M et al (eds) Proceedings of the ocean drilling program, scientific results. Ocean Drilling Program, College Station, 159, pp. 93–99.

Boadi, B., Wemegah, D. D., Preko, K. 2013. Geological and Structural Interpretation of the Konongo Area of the Ashanti Gold Belt of Ghana from Aeromagnetic and Radiometric data. International Research Journal of Geology and Mining, 3(3), pp. 124-135.

Ejepu, J. S., Unuevho, C. I., Ako, T. A., Abdullahi, S. 2018. Integrated geosciences prospecting for gold mineralisation in Kwakuti, North-Central, Nigeria. Journal of Geology and Mining Research, 10(7), pp. 81-94.

Elkhateeb, S. O., Abdellatif, M. A. G. 2018. Delineation potential gold mineralization zones in a part of Central Eastern Desert, Egypt using Airborne Magnetic and Radiometric data. NRIAG Journal of Astronomy and Geophysics, 7, pp. 361-376.

Hoover, D. B., Pierce, H. A. 1990. Annotated Bibliography of Gamma-Ray Methods Applied to Gold Exploration. U.S.G.S. Open-File Report, pp. 90-203, 23.

International Atomic Energy Agency. 2003. Guidelines for radioelement mapping using Gamma ray spectrometry data, Vienna.

Ishalu, G., Tsepav, M.T. 2018. Interpretation of Ground Magnetic data, over suspected Gold deposit in Gwam. International Journal of Advances in Scientific Research and Engineering.

Jaques, A. L., Wellman, P., Whitaker, A., Wyborn, D. 1997. High-resolution Geophysics in Modern geological mapping. Journal of Australia Geology Geophysics, 17, pp. 159– 173.

Obaje, N. G. 2009. Geology and Mineral Resources of Nigeria, Lecture Notes in the Earth Science Springer: Heidelberg.

Salawu, N. B., Fatoba, J. O., Adebiyi, L. S., Eluwole, A. B., Olasunkanmi, N. K., Orosun, M. M., Dada S. S. 2021. Structural geometry of Ikogosi warm spring, Southwestern Nigeria: evidence from aeromagnetic and remote sensing interpretation. Geomechanics Geophysics Geo-energy Geo-resources.7, pp. 26. DOI: https://doi.org/10.1007/s40948-021-00224-x(0123456789.

Saleh, A., Qudus, B., Magawata, Z. U., Augie, A. I. 2020. Delineation of structural features and depth to the magnetic sources over Allawa and its environs, Northcentral Nigeria. International Journal of Advances in Engineering and Management (IJAEM), 2(6), pp. 545-553.

Sillitoe, R. H. 1999. Style of High Sulphidation Gold, Silver, and Copper Mineralisation in Porphyry and Epithermal Environments. Proceeding PACRIM Congress, Bali.

Silva, A. M., Pires, A. C. B., McCafferty, A., Moraes, R. A. V., Xia, H. 2003. Application of Airborne geophysical data to mineral exploration in the uneven exposed terrains of the Rio Das Velhas greenstone belt. Revista Brasileira de Geociências, 33(2), pp. 17–28.

Telford, W. M., Geldart, L. P., Sheriff, R. E. 1990. Applied Geophysics. Cambridge University Press, second edition.

Thompson D. T. 1982. EULDPH: a new technique for making computer assisted depth estimates from magnetic data. Geophysics, 47(1), pp. 31-37.

Wemegah, D. D., Preko, K., Noye, R.M., Boadi, B., Menyeh, A., Danuor, S.K., Amenyoh T. 2015. Geophysical Interpretation of Possible Gold Mineralization Zones in Kyerano, South-Western Ghana: Using Aeromagnetic and Radiometric Datasets. Journal of Geoscience and Environment Protection, 3, pp. 67-82.

Woakes, M., Rahaman, M.A., Ajibade, A. C. 1987. Some metallogenetic features of the Nigerian Basement. Journal of African Earth Science, 6, pp. 54–64.